



Since January 2020 Elsevier has created a COVID-19 resource centre with free information in English and Mandarin on the novel coronavirus COVID-19. The COVID-19 resource centre is hosted on Elsevier Connect, the company's public news and information website.

Elsevier hereby grants permission to make all its COVID-19-related research that is available on the COVID-19 resource centre - including this research content - immediately available in PubMed Central and other publicly funded repositories, such as the WHO COVID database with rights for unrestricted research re-use and analyses in any form or by any means with acknowledgement of the original source. These permissions are granted for free by Elsevier for as long as the COVID-19 resource centre remains active.

# Detection of Different COVID-19 Pneumonia Phenotypes with Estimated Alveolar Collapse and Overdistention by Bedside Electrical Impedance Tomography<sup>\*</sup>

Rongqing Chen<sup>\*</sup> Andrés Lovas<sup>\*\*</sup> Balázs Benyó<sup>\*\*\*</sup>  
Knut Möller<sup>\*</sup>

<sup>\*</sup> Institute of Technical Medicine, Furtwangen University,  
Jakob-Kienzle-Str. 17, VS-Schwenningen, Germany (e-mail:  
[rongqing.chen@hs-furtwangen.de](mailto:rongqing.chen@hs-furtwangen.de)).

<sup>\*\*</sup> Kiskunhalas Semmelweis Hospital, Department of Anaesthesiology  
and Intensive Therapy, H-6400, Dr. Monzpart L. u. 1, Hungary

<sup>\*\*\*</sup> Department of Control Engineering and Information Technology,  
Budapest University of Technology and Economics, 1117 Budapest,  
Magyar tudósok krt. 2, Hungary

**Abstract:** COVID-19 induced acute respiratory distress syndrome (ARDS) could have two different phenotypes, which was reported to have different response and outcome to the typical ARDS positive end-expiratory pressure (PEEP) treatment. The identification of the different phenotypes in terms of the recruitability can help improve the patient outcome. In this contribution we conducted alveolar overdistention and collapse analysis with the long term electrical impedance tomography monitoring data on two severe COVID-19 pneumonia patients. The result showed different patient reactions to the PEEP trial, revealed the progressive change in the patient status, and indicted a possible phenotype transition in one patient. It might suggest that EIT can be a practical tool to identify phenotypes and to provide progressive information of COVID-19 pneumonia.

Copyright © 2021 The Authors. This is an open access article under the CC BY-NC-ND license (<https://creativecommons.org/licenses/by-nc-nd/4.0/>)

**Keywords:** biomedical imaging systems; decision support systems for the control of physiological and clinical variables; control of voluntary movements, respiration, locomotion

## 1. INTRODUCTION

A large proportion of severe respiratory failure cases of COVID-19 pneumonia fulfill the Berlin definition of acute respiratory distress syndrome (ARDS) (Grasselli et al., 2020; Arabi et al., 2020; Wu et al., 2020; The ARDS Definition Task Force<sup>\*</sup>, 2012). Despite sharing the same etiology, the COVID-19 patients were observed with different characteristics. It is reported that more than 50% of the patients were observed with severe hypoxemia, but with a near normal respiratory system compliance (Gattinoni et al., 2020a). These patients were lately categorized as L-type patients characterized by low elastance, low ventilation-to-perfusion (VA/Q) ratio, low lung weight and low recruitability. In contrast, there exist H-type patients who have high elastance, high ventilation-to-perfusion (VA/Q) ratio, high lung weight and high recruitability (Gattinoni et al., 2020a). The reaction of the L-type patients to the positive end-expiratory pressure (PEEP) trial, a traditional ARDS treatment, is not as good as that of H-type patients. Sometimes the higher PEEP might

induce lung injuries which will eventually compromise the outcome. Instead of following the treatment recommendations for ARDS patients (Alhazzani et al., 2020), concerns arisen that L-type COVID-19 pneumonia is of pathophysiology and should be treated as a different disease (Gattinoni et al., 2020a,b,c). A common method to identify the different COVID-19 pneumonia phenotype is through CT scans (GECOVID (GENoa COVID-19) group et al., 2021). However, the course of the COVID-19 pneumonia has shown to develop very fast. It is reported that some COVID-19 pneumonia patients had low recruitability even though large amount of non-aerated tissue was observed and the compliance was fairly low (Zhao et al., 2020). The possible phenotype transitions from L-Type to H-Type were reported by different authors (Gattinoni et al., 2020b; Camporota et al., 2020; for the COVADIS study group et al., 2021). Daily CT scans on a severe COVID-19 patient is not practical. It is suggested that physiological properties can be used as surrogates to identify L-type and H-type patients, for example the respiratory system compliance and the response to PEEP (recruitability). Other available lung imaging techniques should also be considered to assist clinicians better in assessing the alterations in critically ill COVID-19 pneumo-

<sup>\*</sup> This research was partly supported by the German Federal Ministry of Education and Research (MOVE, Grant 13FH628IX6) and H2020 MCSA Rise (#872488 DCPM).

nia patients(GECOVID (GEnoa COVID-19) group et al., 2021).

Electrical impedance tomography (EIT) is a radiation-free functional image modality which have been clinically proven in terms of monitoring regional lung effects in mechanically ventilated patients with ARDS. EIT is capable of identifying overdistention or collapse in the dependent part during PEEP trial(Costa et al., 2009). The result agreed well with that calculated from CT data. Zhao et al. also suggested that the EIT bedside monitoring can play an important role to detect the different phenotypes of the COVID-19 pneumonia in addition to CT examination(Zhao et al., 2020).

The objective of this work is to show the insight of a possible method to provide supplementary information for the COVID-19 pneumonia diagnosis and its developing course in terms of recruitable alveolar collapse and overdistention ratio during the PEEP trial on two severe COVID-19 patients admitted to intensive care unit (ICU). One patient was monitored by EIT device for seven days, and the other patient for even twelve days. Cumulative collapse and overdistention ratio were calculated and compared at each PEEP step.

## 2. METHOD

### 2.1 Patient data

The study was approved by the Human Investigation Review Board of the University of Szeged with approval number 67/2020-SZTE. The trial was registered on ClinicalTrials.gov under NCT04360837. Written informed was obtained from the patients or their legal representatives. To follow the pathological development over at least a week, we included 2 patients both diagnosed with COVID-19 pneumonia into this evaluation. The COVID-19 pneumonia patient A is female, 67 years old, with hypothyreosis and hypertension in the past medical history; the COVID-19 pneumonia patient B is female, 81 years old, with hypertension in the past medical history. Further details on the studied patients are shown in table 1. Both patients were deep sedated, intubated and ventilated. The ventilator was operated in pressure-controlled mode with a constant pressure increment of 15 cmH<sub>2</sub>O above PEEP during inspiration. A PEEP trial maneuver with an incremental and a decremental limb was conducted daily on both patients. During the incremental part, a 3 cmH<sub>2</sub>O stepwise increase in airway pressure from 10 cmH<sub>2</sub>O to the maximum pressure of 25 cmH<sub>2</sub>O were applied leading to an overall peak pressure of 40 cmH<sub>2</sub>O. In the decremental limb, in steps of 3 cmH<sub>2</sub>O the PEEP was reduced from the maximum of 25 cmH<sub>2</sub>O to the minimum pressure of 10 cmH<sub>2</sub>O. On each PEEP level PEEP was kept constant for two minutes with ongoing ventilation. The patient A was monitored for seven days, while the patient B was investigated for twelve days.

The EIT measurement was performed with a Dräger PulmoVista 500 device (Dräger Medical, Lübeck, Germany). The device has 16 electrodes equidistantly placed on chest circumference in a transverse plane between the 5th and 6th intercostal space. EIT monitoring data were measured with adjacent injection current and adjacent voltage measurement with 50 frames per second. Time difference

EIT images were reconstructed using the Newton-Raphson algorithm.

### 2.2 Pixel compliance

The calculation of the pixel compliance requires the knowledge of the inhaled amount of air inside the corresponding lung compartment (regional tidal volume) and the driving pressure. In this contribution, as the patients were ventilated in a pressure control mode, the difference between the plateau pressure and PEEP can be a substitute of the driving pressure. This approximation was made under the condition that both end-inspiration flow and end-expiration flow were zero, for example, the alveolar and proximal pressure are equal. The regional tidal volume can be estimated by the related pixel value of an EIT tidal image. It is reported that the regional tidal volume correlates well with the pixel wise conductivity variation ( $\Delta Z$ ) shown by the EIT tidal image(Victorino et al., 2004; Frerichs et al., 2001, 2002; Leonhardt and Lachmann, 2012). Therefore, the pixel compliance can be calculated as:

$$Compliance_{pixel} = \frac{\Delta Z}{P_{plateau} - PEEP} \quad (1)$$

Considering the fact that the gravitational forces increase perfusion in the dependent parts of lung, the corresponding plateau pressure should be larger(Ochiai, 2015). Thus, the driving pressure at the airway opening should not be a constant in the entire lung area. The lung area can be horizontally segmented to different layers with different plateau pressures, for example in Fig. 1a the lung area is divided to  $m$  layers. In this contribution, there were eight layers of different plateau pressures. Both patients were ventilated in supine position where the tracheal tube is located in the same plane as the ventral lung. The measured plateau pressure was considered equal to the  $P_{plateau}^1$  at the layer 1. The  $P_{plateau}^n$  ( $n \leq 8$ ) at layer  $n$  was set to be 2 cmH<sub>2</sub>O larger than the plateau pressure at layer  $n-1$ .

### 2.3 Estimation of collapse and overdistention

In a decremental PEEP trial, a relief of the overdistention area might be observed, while other recruited area might undergo collapse. The relief of overdistention is observed with an increase of pixel compliance, while the collapse a decrease of pixel compliance. Thus, in a PEEP trial, the pixel compliance can be observed with opposite behaviors, e.g. the compliance curve in Fig. 1b. It is assumed that the regional lung reaches the best compliance when the corresponding pixel compliance is the largest as shown in Fig. 1b. With this assumption, Costa et al. designed an algorithm that can estimate the cumulative collapse and overdistention ratio in a decremental PEEP trial:

- (1) using 1 to calculate every pixel compliance at each PEEP step;
- (2) for each pixel at each PEEP level, the pixel collapse ratio can be calculated as:

$$collapse_{px} = \frac{best\ compl_{px} - current\ compl_{px}}{best\ compl_{px}} \quad (2)$$

Table 1. Characteristics of investigated COVID-19 pneumonia patients

Patient Ref.	Gender	Age, yr	BMI, kg/m <sup>2</sup>	APACHE II	RASS Scale	Days of trial
A	Female	67	29.7	17	-4	7
B	Female	81	31.2	18	-5	12

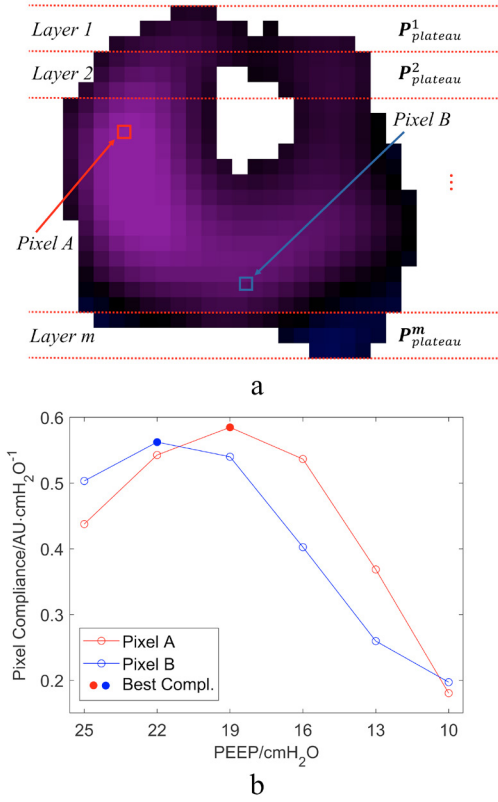


Fig. 1. (a) An example of a lung area segmented to  $m$  layers with different plateau pressures, where pixel A and pixel B are at different layers; (b) Respective pixel compliance of pixel A and B during a decremental PEEP trial, where the best pixel compliance are reached at different PEEP steps

where the  $best\ compl_{px}$  is determined as the largest compliance of the corresponding pixel,  $current\ compl_{px}$  is the corresponding pixel compliance at current PEEP, the collapse ratio is set to 0 when the best compliance has not been reached at the current PEEP step;

- (3) the cumulated collapse ratio for the entire lung area at each PEEP step can be calculated by the weighted average of the pixel collapse ratio. The weight is the best pixel compliance:

$$collapse_{cumu} = \frac{\sum(collapse_{px} \times best\ compl_{px})}{\sum best\ compl_{px}} \quad (3)$$

where the  $\sum(collapse_{px} \times best\ compl_{px})$  and  $\sum best\ compl_{px}$  sum all the pixels within the lung area;

- (4) similarly, the pixel overdilation ratio at each PEEP step can be calculated as:

$$overdist_{px} = \frac{best\ compl_{px} - current\ compl_{px}}{best\ compl_{px}} \quad (4)$$

where the  $best\ compl_{px}$  is determined as the largest compliance of the corresponding pixel,

$current\ compl_{px}$  is the corresponding pixel compliance at current PEEP, the overdilation ratio is set to 0 when the best compliance has already been reached at the current PEEP step;

- (5) the cumulated overdilation ratio for the entire lung area at each PEEP step can be calculated by the weighted average of the pixel overdilation ratio. The weight is the best pixel compliance:

$$overdist_{cumu} = \frac{\sum(overdist_{px} \times best\ compl_{px})}{\sum best\ compl_{px}} \quad (5)$$

where the  $\sum(overdist_{px} \times best\ compl_{px})$  and  $\sum best\ compl_{px}$  sum all the pixels within the lung area.

### 3. RESULTS

An example of pixel collapse and overdilation ratio images of first day of the investigated COVID-19 pneumonia patients estimated by the described algorithm are shown in Fig. 2 respectively. The results of the Patient A were shown in the first row, Patient B the second row. Red areas indicated the corresponding lung area that was found to be overdilated, while the collapse area was depicted in blue. The results comply with the fact that collapse or derecruitment were expected at dependent lung parts at a lower PEEP step, while overdilation at the ventral lung area at a higher PEEP step. The cumulative overdilation ratio for both patients was similar at the first day, but the cumulative collapse ratio was larger and increased faster when PEEP was decreased for Patient A at the first day.

The cumulative overdilation ratio and the cumulative collapse ratio for each patient at different PEEP steps on each day are shown respectively in table 2 and table 3. The overdilation ratio at the highest PEEP level (25 cmH<sub>2</sub>O) and the collapse ratio at the lowest PEEP (10 cmH<sub>2</sub>O) of each patient are depicted in Fig. 3 respectively.

In table 2, it was shown that the cumulative overdilation ratio decreased in the decremental PEEP trial. Nearly no overdilation was observed at the PEEP 13 cmH<sub>2</sub>O for both patients. In Fig. 3, Patient A shows an increasing trend of cumulative overdilation ratio at the PEEP 25 cmH<sub>2</sub>O during the seven-day monitoring, while for Patient B the cumulative overdilation ratio at the PEEP 25 cmH<sub>2</sub>O was fluctuating. For both patients, the cumulative overdilation ratio at the PEEP 25 cmH<sub>2</sub>O was greater than 0.2.

Table 3 indicates that the cumulative collapse ratio increased in the decremental PEEP trial. For both patients, the collapse was observed from PEEP 19 cmH<sub>2</sub>O, but very minor at this PEEP setting. Patient A witnessed a steeper increasing trend of the collapse ratio than Patient B at PEEP 10 cmH<sub>2</sub>O, Patient A shows a larger collapse ratio in Fig. 3. It is worth noting that the cumulative collapse ratio at the PEEP 10 cmH<sub>2</sub>O of Patient A witnessed a decreasing trend over time.

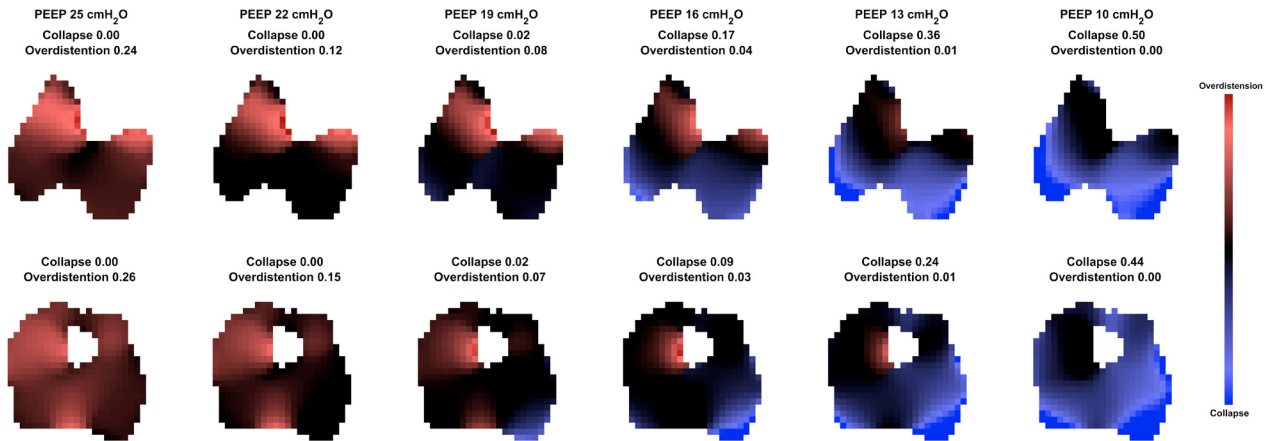


Fig. 2. An example of pixel collapse and overdistention ratio images of the first day of the investigated COVID-19 pneumonia patients at different decremental PEEP steps. Upper row: Patient A; lower row: Patient B

Table 2. Estimation of cumulative overdistention ratio at each PEEP step

Patient Ref.	Day	PEEP(cmH <sub>2</sub> O)					
		25	22	19	16	13	10
A	1	0.24	0.12	0.08	0.04	0.01	0.00
	2	0.32	0.17	0.10	0.05	0.01	0.00
	3	0.35	0.15	0.06	0.02	0.00	0.00
	4	0.36	0.20	0.09	0.03	0.01	0.00
	5	0.40	0.24	0.13	0.05	0.01	0.00
	6	0.42	0.24	0.10	0.02	0.00	0.00
	7	0.48	0.23	0.10	0.04	0.01	0.00
B	1	0.26	0.15	0.07	0.03	0.01	0.00
	2	0.32	0.19	0.10	0.03	0.01	0.00
	3	0.39	0.27	0.15	0.05	0.00	0.00
	4	0.27	0.16	0.08	0.06	0.04	0.00
	5	0.40	0.16	0.03	0.02	0.01	0.00
	6	0.38	0.21	0.09	0.04	0.02	0.00
	7	0.34	0.20	0.13	0.06	0.02	0.00
	8	0.38	0.21	0.13	0.07	0.02	0.00
	9	0.23	0.11	0.04	0.01	0.00	0.00
	10	0.42	0.28	0.17	0.04	0.01	0.00
	11	0.35	0.19	0.12	0.07	0.02	0.00
	12	0.41	0.28	0.20	0.08	0.04	0.00

Table 3. Estimation of cumulative collapse ratio at each PEEP step

Patient Ref.	Day	PEEP(cmH <sub>2</sub> O)					
		25	22	19	16	13	10
A	1	0.00	0.00	0.02	0.17	0.36	0.50
	2	0.00	0.00	0.02	0.12	0.27	0.45
	3	0.00	0.00	0.01	0.07	0.20	0.42
	4	0.00	0.00	0.02	0.09	0.24	0.46
	5	0.00	0.00	0.00	0.04	0.15	0.32
	6	0.00	0.00	0.01	0.04	0.14	0.33
	7	0.00	0.00	0.00	0.04	0.14	0.31
B	1	0.00	0.00	0.02	0.09	0.24	0.44
	2	0.00	0.00	0.00	0.04	0.12	0.31
	3	0.00	0.00	0.02	0.05	0.17	0.33
	4	0.00	0.00	0.02	0.10	0.15	0.23
	5	0.00	0.00	0.00	0.09	0.22	0.35
	6	0.00	0.00	0.00	0.04	0.13	0.31
	7	0.00	0.00	0.02	0.04	0.13	0.20
	8	0.00	0.00	0.02	0.07	0.17	0.25
	9	0.00	0.00	0.01	0.08	0.20	0.35
	10	0.00	0.00	0.00	0.01	0.07	0.23
	11	0.00	0.00	0.01	0.04	0.19	0.30
	12	0.00	0.00	0.01	0.03	0.08	0.18

#### 4. DISCUSSION

Two severe COVID-19 pneumonia patients were monitored with EIT and analysed by the cumulative overdistention or collapse ratio. The result might suggest that Patient A is not as recruitable as Patient B. With additional medical information which states Patient A had high respiratory system compliance while Patient B low respiratory system compliance, Patient A is a L-type patient, while Patient B is a H-type patient. A possible transition from the L-type patient to the H-type could be observed as the cumulative collapse ratio at the lowest PEEP step decreased over time in addition to the respiratory system compliance deterioration.

Transition of the patient from Type L to Type H might be ascribed to the evolution of the COVID-19 pneumonia on one hand and to the lung injury attributable to high-stress ventilation on the other (Gattinoni et al., 2020a). Thus, it is suggested that high PEEP level should be avoiding in critically ill patients with severe COVID-19 pneumonia to reduce the possibility of worsened respi-

ratory mechanics (GECOVID (Genoa COVID-19) group et al., 2021). However, the H-type COVID-19 pneumonia patients are still profiting from a high PEEP strategy (Cammarota et al., 2021). In addition, it is confirmed that L-type patients react better in terms of the reversed hypoxemia by an increase in FiO<sub>2</sub> when compared to the PEEP approach. From the reported cases (Gattinoni et al., 2020a). An accurate diagnosis of the COVID-19 pneumonia phenotype is crucial to determine the proper treatment that benefits the patient reaction and outcome. Our research suggests that EIT is capable of diagnosing COVID-19 pneumonia phenotype.

There still exist other approaches capable of phenotype diagnosis: COVID-19 pneumonia phenotypes could be diagnosed with a recruitment-to-inflation ratio (R/I ratio), but this protocol only supports volume control ventilation and requires extra single-breath experiments (Beloncle et al., 2020). CT scans and corresponding Hounsfield unit histograms are available for diagnosis (Gattinoni et al., 2020a), but this cannot provide progressive information as continuous CT scans are not ethical. The estimation

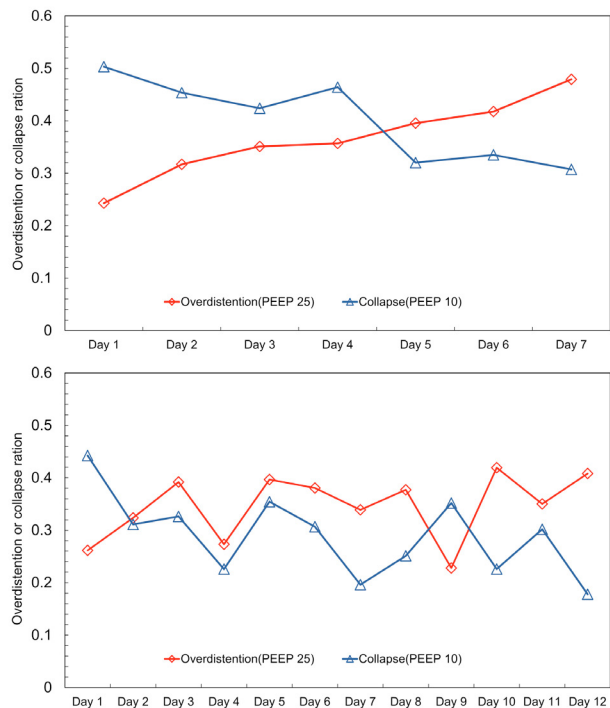


Fig. 3. The overdistention ratio at the highest PEEP level (25 cmH<sub>2</sub>O) and the collapse ratio at the lowest PEEP (10 cmH<sub>2</sub>O) for each patient on each day. Red diamond: overdistention ratio (PEEP 25 cmH<sub>2</sub>O); blue triangle: collapse ratio (PEEP 10 cmH<sub>2</sub>O). Upper row: Patient A; lower row: Patient B

of cumulative overdistention and collapse ratio from the EIT data can reveal the reaction of ARDS patients to the PEEP trial and provide progressive patient status information. EIT might develop into a useful and practical tool to assist with the bedside monitoring of COVID-19 patients in addition to CT scans.

One of the limitations of this research is that we estimated a completely aerated lung after the incremental PEEP trial. With this estimation we calculated the relative ratio of the recruitable alveolar collapse. This is a limitation of the time difference EIT protocol as an absolute amount of collapse cannot be obtained. Nevertheless, this protocol still yields a collapse ratio related to the minimum possible collapse, but can still provide information of the patient status. The other limitation is that we have not obtained all medical characteristics of both patients due to the pandemic severity, otherwise more comparison and validation could be done.

The estimation of recruitable alveolar overdistention and collapse calculated from EIT bedside monitoring data indeed provides progressive information, including the whole lung status and regional lung behavior, and can be generated in real-time during the mechanical ventilation. In addition to the CT golden standard, EIT could be an assistive method providing clinicians with bedside continuous monitoring containing direct pathophysiological information.

## 5. CONCLUSION

The course of the COVID-19 pneumonia is still poorly understood and has shown to develop very fast. In this contribution, an EIT-based estimation method in terms of alveolar overdistention and collapse was presented and implemented on two severe COVID-19 pneumonia patients. The result shows different reactions of the patients to a PEEP trial, and might suggest a transition of a patient between different phenotypes. EIT might develop into a useful and practical tool to assist with the classification of the different phenotypes of the COVID-19 patients in addition to the CT scans, and might provide additional information of the disease facilitating the evaluation of the respective treatments.

## REFERENCES

- Alhazzani, W., Møller, M.H., Arabi, Y.M., Loeb, M., Gong, M.N., Fan, E., Oczkowski, S., Levy, M.M., Derde, L., Dzierba, A., Du, B., Aboodi, M., Wunsch, H., Cecconi, M., Koh, Y., Chertow, D.S., Maitland, K., Alshamsi, F., Belley-Cote, E., Greco, M., Laundry, M., Morgan, J.S., Kesecioglu, J., McGeer, A., Mermel, L., Mammen, M.J., Alexander, P.E., Arrington, A., Centofanti, J.E., Citerio, G., Baw, B., Memish, Z.A., Hammond, N., Hayden, F.G., Evans, L., and Rhodes, A. (2020). Surviving Sepsis Campaign: Guidelines on the management of critically ill adults with Coronavirus Disease 2019 (COVID-19). *Intensive Care Medicine*, 46(5), 854–887. doi:10.1007/s00134-020-06022-5.
- Arabi, Y.M., Murthy, S., and Webb, S. (2020). COVID-19: A novel coronavirus and a novel challenge for critical care. *Intensive Care Medicine*, 46(5), 833–836. doi:10.1007/s00134-020-05955-1.
- Beloncle, F.M., Pavlovsky, B., Desprez, C., Fage, N., Olivier, P.Y., Asfar, P., Richard, J.C., and Mercat, A. (2020). Recruitability and effect of PEEP in SARS-Cov-2-associated acute respiratory distress syndrome. *Annals of Intensive Care*, 10(1), 55. doi:10.1186/s13613-020-00675-7.
- Cammarota, G., Simonte, R., and De Robertis, E. (2021). PEEP-induced alveolar recruitment in patients with COVID-19 pneumonia: Take the right time! *Critical Care*, 25(1), 163. doi:10.1186/s13054-021-03573-x.
- Camporota, L., Vasques, F., Sanderson, B., Barrett, N.A., and Gattinoni, L. (2020). Identification of pathophysiological patterns for triage and respiratory support in COVID-19. *The Lancet Respiratory Medicine*, 8(8), 752–754. doi:10.1016/S2213-2600(20)30279-4.
- Costa, E.L.V., Borges, J.B., Melo, A., Suarez-Sipmann, F., Toufen, C., Bohm, S.H., and Amato, M.B.P. (2009). Bedside estimation of recruitable alveolar collapse and hyperdistension by electrical impedance tomography. *Intensive Care Medicine*, 35(6), 1132–1137. doi:10.1007/s00134-009-1447-y.
- for the COVADIS study group, Vandenberg, B., Ehrmann, S., Piagnerelli, M., Sauneuf, B., Serck, N., Soumagne, T., Textoris, J., Vinsonneau, C., Aissaoui, N., Blonz, G., Carbutti, G., Courcelle, R., D’hondt, A., Gaudry, S., Higny, J., Horlait, G., Hraiech, S., Lefebvre, L., Lejeune, F., Ly, A., Lascarrou, J.B., and Grimaldi, D. (2021). Static compliance of the respiratory system in COVID-19 related ARDS: An international multicenter

- study. *Critical Care*, 25(1), 52. doi:10.1186/s13054-020-03433-0.
- Frerichs, I., Schiffmann, H., Hahn, G., and Hellige, G. (2001). Non-invasive radiation-free monitoring of regional lung ventilation in critically ill infants. *Intensive Care Medicine*, 27(8), 1385–1394. doi:10.1007/s001340101021.
- Frerichs, I., Hinz, J., Herrmann, P., Weisser, G., Hahn, G., Dudykevych, T., Quintel, M., and Hellige, G. (2002). Detection of local lung air content by electrical impedance tomography compared with electron beam CT. *Journal of Applied Physiology (Bethesda, Md.: 1985)*, 93(2), 660–666. doi:10.1152/jappphysiol.00081.2002.
- Gattinoni, L., Chiumello, D., Caironi, P., Busana, M., Romitti, F., Brazzi, L., and Camporota, L. (2020a). COVID-19 pneumonia: Different respiratory treatments for different phenotypes? *Intensive Care Medicine*, 46(6), 1099–1102. doi:10.1007/s00134-020-06033-2.
- Gattinoni, L., Chiumello, D., and Rossi, S. (2020b). COVID-19 pneumonia: ARDS or not? *Critical Care (London, England)*, 24(1), 154. doi:10.1186/s13054-020-02880-z.
- Gattinoni, L., Coppola, S., Cressoni, M., Busana, M., Rossi, S., and Chiumello, D. (2020c). COVID-19 Does Not Lead to a “Typical” Acute Respiratory Distress Syndrome. *American Journal of Respiratory and Critical Care Medicine*, 201(10), 1299–1300. doi:10.1164/rccm.202003-0817LE.
- GECOVID (Genoa COVID-19) group, Ball, L., Robba, C., Maiello, L., Herrmann, J., Gerard, S.E., Xin, Y., Battaglini, D., Brunetti, I., Minetti, G., Seitun, S., Vena, A., Giacobbe, D.R., Bassetti, M., Rocco, P.R.M., Cereda, M., Castellan, L., Patroniti, N., and Pelosi, P. (2021). Computed tomography assessment of PEEP-induced alveolar recruitment in patients with severe COVID-19 pneumonia. *Critical Care*, 25(1), 81. doi:10.1186/s13054-021-03477-w.
- Grasselli, G., Zangrillo, A., Zanella, A., Antonelli, M., Cabrini, L., Castelli, A., Cereda, D., Coluccello, A., Foti, G., Fumagalli, R., Iotti, G., Latronico, N., Lorini, L., Merler, S., Natalini, G., Piatti, A., Ranieri, M.V., Scandroglio, A.M., Storti, E., Cecconi, M., Pesenti, A., COVID-19 Lombardy ICU Network, Agosteo, E., Alaimo, V., Albano, G., Albertin, A., Alborghetti, A., Aldegheri, G., Antonini, B., Barbara, E., Belgiorno, N., Belliato, M., Benini, A., Beretta, E., Bianciardi, L., Bonazzi, S., Borelli, M., Boselli, E., Bronzini, N., Capra, C., Carnevale, L., Casella, G., Castelli, G., Catena, E., Cattaneo, S., Chiumello, D., Cirri, S., Citerio, G., Colombo, S., Coppini, D., Corona, A., Cortellazzi, P., Costantini, E., Covello, R.D., De Filippi, G., Dei Poli, M., Della Mura, F., Evasi, G., Fernandez-Olmos, R., Forastieri Molinari, A., Galletti, M., Gallioli, G., Gemma, M., Gnesin, P., Grazioli, L., Greco, S., Gritti, P., Grosso, P., Guatteri, L., Guzzon, D., Harizay, F., Keim, R., Landoni, G., Langer, T., Lombardo, A., Malara, A., Malpetti, E., Marino, F., Marino, G., Mazzone, M.G., Merli, G., Micucci, A., Mojoli, F., Muttini, S., Nailescu, A., Panigada, M., Perazzo, P., Perego, G.B., Petrucci, N., Pezzi, A., Protti, A., Radrizzani, D., Raimondi, M., Ranucci, M., Rasulo, F., Riccio, M., Rona, R., Roscitano, C., Ruggeri, P., Sala, A., Sala, G., Salvi, L., Sebastiano, P., Severgnini, P., Sforzini, I., Sigurtà, F.D., Subert, M., Tagliabue, P., Troiano, C., Valsecchi, R., Viola, U., Vitale, G., Zambon, M., and Zoia, E. (2020). Baseline Characteristics and Outcomes of 1591 Patients Infected With SARS-CoV-2 Admitted to ICUs of the Lombardy Region, Italy. *JAMA*, 323(16), 1574. doi:10.1001/jama.2020.5394.
- Leonhardt, S. and Lachmann, B. (2012). Electrical impedance tomography: The holy grail of ventilation and perfusion monitoring? *Intensive Care Medicine*, 38(12), 1917–1929. doi:10.1007/s00134-012-2684-z.
- Ochiai, R. (2015). Mechanical ventilation of acute respiratory distress syndrome. *Journal of Intensive Care*, 3(1). doi:10.1186/s40560-015-0091-6.
- The ARDS Definition Task Force\* (2012). Acute Respiratory Distress Syndrome: The Berlin Definition. *JAMA*, 307(23), 2526–2533. doi:10.1001/jama.2012.5669.
- Victorino, J.A., Borges, J.B., Okamoto, V.N., Matos, G.F.J., Tucci, M.R., Carames, M.P.R., Tanaka, H., Sipmann, F.S., Santos, D.C.B., Barbas, C.S.V., Carvalho, C.R.R., and Amato, M.B.P. (2004). Imbalances in regional lung ventilation: A validation study on electrical impedance tomography. *American Journal of Respiratory and Critical Care Medicine*, 169(7), 791–800. doi:10.1164/rccm.200301-133OC.
- Wu, C., Chen, X., Cai, Y., Xia, J., Zhou, X., Xu, S., Huang, H., Zhang, L., Zhou, X., Du, C., Zhang, Y., Song, J., Wang, S., Chao, Y., Yang, Z., Xu, J., Zhou, X., Chen, D., Xiong, W., Xu, L., Zhou, F., Jiang, J., Bai, C., Zheng, J., and Song, Y. (2020). Risk Factors Associated With Acute Respiratory Distress Syndrome and Death in Patients With Coronavirus Disease 2019 Pneumonia in Wuhan, China. *JAMA Internal Medicine*, 180(7), 934. doi:10.1001/jamainternmed.2020.0994.
- Zhao, Z., Kung, W.H., Chang, H.T., Hsu, Y.L., and Frerichs, I. (2020). COVID-19 pneumonia: Phenotype assessment requires bedside tools. *Critical Care*, 24. doi:10.1186/s13054-020-02973-9.